PROCEEDINGS of the
23rd International Congress on Acoustics
9 to 13 September 2019 in Aachen, Germany

The acoustic absorption coefficient of short circular holes sustaining a high Reynolds number bias flow

Renaud GAUDRON[(1)], Aimee S. MORGANS[(2)]

[(1)]Department of Mechanical Engineering, Imperial College London, UK, r.gaudron@imperial.ac.uk
[(2)]Department of Mechanical Engineering, Imperial College London, UK

Abstract

The damping of acoustic waves across short circular holes sustaining a high Reynolds number bias flow is of interest in many engineering applications, such as aircraft and rocket engines liners. This damping is generated by the interaction between acoustic waves and unsteady vortical structures generated at the perforation rim. The objective of this work is to determine and compare the acoustic absorption coefficient of a short circular hole sustaining a high Reynolds number, low Mach number bias flow for two distinct models. In the first model, the acoustic response of the hole is described using an isentropic area decrease followed by a non-isentropic area increase with large scale flow separation. In the second model, the acoustic response of the hole is described using Howe's model assuming that the incoming perturbations are hydrodynamically compact. For both models, the acoustic absorption coefficient is shown to depend on the cross section area ratio θ, Mach number inside the hole M_2 and upstream boundary acoustic reflection coefficient $\mathcal{R}_1$ only. For limited values of θ and M_2, the acoustic absorption coefficient remains close to zero and does not depend on $\mathcal{R}_1$. On the other hand, for large values of θ and M_2, the acoustic absorption coefficient is found to be highly dependent on $\mathcal{R}_1$ and may become close to unity, thus indicating that a large fraction of the incoming acoustic energy is damped across the hole for such parameters.

Keywords: Acoustic absorption, Short circular holes

1 INTRODUCTION

Short circular holes and perforated plates are used for their acoustic damping properties in many engineering applications, ranging from thermoacoustic instability control using perforated liners in aero-engines or land-based gas turbines [1, 13, 14] to broadband noise absorption in car mufflers [12]. In most cases, these short circular holes sustain a high Reynolds number bias flow which significantly affects the acoustic energy balance of the system [6, 11, 15]. The main objective of this work is to predict the acoustic absorption coefficient [9, 10] of short circular holes sustaining a high Reynolds number, low Mach number bias flow based on two analytical models widely employed in low order network tools used for thermoacoustic stability prediction [4, 7].

The geometry of interest and the corresponding mean flow considerations are first examined in Sec. 2. Two analytical models predicting the acoustic absorption coefficient generated by a short circular hole sustaining a high Reynolds number, low Mach number bias flow are then derived in Sec. 3. The first analytical model, called the 2-step (2S) model and consisting of an isentropic area decrease followed by an area increase with large scale flow separation, is investigated in Sec. 3.1. The second analytical model, called the quasi-steady Howe's (QSH) model and accounting for the interaction between vortical structures generated at the burner rim and sound waves, is investigated in Sec. 3.2. The analytical predictions of the acoustic absorption coefficient according to these two models are then discussed in Sec. 4.

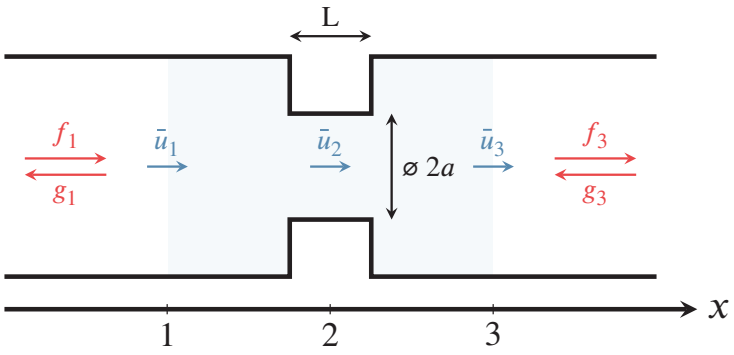

Figure 1. Sketch representing the hole geometry. The mean flow direction is from left to right.

2 PROBLEM SETTING

The scope of this work is limited to the absorption of linear acoustic waves across single short circular holes sustaining a high Reynolds number, low Mach number bias flow. The fluid is assumed to be a perfect gas. The geometry of interest, represented in Fig. 1, is assumed to be axisymmetric. The single circular perforation has a length L and a radius a and both the upstream and downstream cross section areas are equal to A. Three reference locations are subsequently defined. The upstream (respectively downstream) reference location is denoted by 1 (respectively 3) while the reference location inside the perforation is denoted by 2. Each variable x_i defined at reference location i can be decomposed into a mean $\bar{x}_i$ and an acoustic x'_i component such that $x'_i \ll \bar{x}_i$. These variables include the gas temperature T, density ρ, pressure p, velocity u and sound speed c. Flow variables are assumed to be one-dimensional in each of these reference sections. The system comprised between section 1 and section 3 is assumed to be acoustically and hydrodynamically compact. The mean flow variables are assumed to be time-independent. Body forces, thermal conduction and thermal radiation are neglected. Entropy waves are not considered in this work. The Riemann invariant associated with sound wave propagation in the flow direction (respectively opposite to the flow) is denoted by f (respectively g). The harmonic convention retained in this article is $\exp(-i\omega t)$ following previous works [6, 15]. Nevertheless, the results presented in Sec. 4 are valid for both harmonic conventions $\exp(\pm i\omega t)$ since the value of the acoustic absorption coefficient does not depend on the harmonic convention.

It can be shown that the mean flow is characterized by eight dimensionless numbers:

$$\begin{array}{llll} M_1 = \bar{u}_1/\bar{c}_1 \quad || & M_3 = \bar{u}_3/\bar{c}_3 \quad || & \alpha_1 = \bar{p}_1/\bar{p}_2 \quad || & \Xi_1 = \bar{c}_1/\bar{c}_2 \\ M_2 = \bar{u}_2/\bar{c}_2 \quad || & \theta = A/\pi a^2 \quad || & \alpha_2 = \bar{p}_2/\bar{p}_3 \quad || & \Xi_2 = \bar{c}_2/\bar{c}_3 \end{array} \tag{1}$$

Where M_i is the mean Mach number at reference location i and α_i (respectively Ξ_i) quantifies the mean pressure (respectively the mean sound speed) ratio between reference locations i and $i+1$. Finally, θ represents the cross section area ratio between reference locations 1 or 3 and reference location 2. The number of dimensionless parameters can be further reduced by considering the mean conservation equations. Accordingly, the mean conservation of mass applied between reference locations 1 and 2 and between reference locations 2 and 3 leads to [5, 8]:

$$M_2 \Xi_1 = \alpha_1 M_1 \theta \tag{2}$$

$$M_3 \Xi_2 \theta = \alpha_2 M_2 \tag{3}$$

Assuming that viscous effects can be neglected at all three reference locations and neglecting terms of order M^2, the mean stagnation enthalpy conservation applied between reference locations 1 and 2 and between reference locations 2 and 3 leads to [5]:

$$\Xi_1 = \Xi_2 = 1 \tag{4}$$

Finally, mean entropy conservation is applied between reference locations 1 and 2 and between reference locations 2 and 3 for the QSH model introduced in Sec. 3.2. The mean flow is assumed to be isentropic throughout the system in that case. On the other hand, for the 2S model introduced in Sec. 3.1, the area increase between reference locations 2 and 3 cannot be assumed to be isentropic because of flow separation [5]. In that case, the mean conservation of momentum is considered between reference locations 2 and 3 [2, 5] and it is assumed that the pressure on the lateral surface just after the sudden cross section area increase is equal to the upstream pressure p_1 [2]. By neglecting terms of order M^2, the mean conservation equations for both models lead to:

$$\alpha_1 = \alpha_2 = 1 \tag{5}$$

In the end, the structure of the mean flow is fully determined by two dimensionless numbers: the Mach number inside the perforation M_2 and the cross section area ratio θ. Furthermore, the mean pressure $\bar{p}$, mean temperature $\overline{T}$, mean sound speed $\bar{c}$ and mean density $\bar{\rho}$ are constant throughout the system.

3 ACOUSTIC ABSORPTION COEFFICIENT

The acoustic absorption coefficient Δ of a compact element located between reference locations i and $i+1$ is a function of the associated S-Matrix (sometimes called Scattering Matrix) $\mathcal{S}_i$, boundary acoustic reflection coefficient $\mathcal{R}_i$ or $\mathcal{R}_{i+1}$, Mach numbers M_i and M_{i+1}, cross section area ratio θ_i, mean pressure ratio α_i and mean sound speed ratio Ξ_i only [5]. For instance, when the upstream acoustic reflection coefficient $\mathcal{R}_i$ is known, the acoustic absorption coefficient is given by [5]:

$$\Delta = 1 - \frac{\left(1+M_{i+1}\right)^2 \left|\mathcal{S}_i(1,2) + \mathcal{R}_i \det \mathcal{S}_i\right|^2 + \theta_i \ \Xi_i \ \alpha_i^{-1} \left(1-M_i\right)^2 \left|\mathcal{S}_i(2,2)\right|^2}{\theta_i \ \Xi_i \ \alpha_i^{-1} \left(1+M_i\right)^2 \left|\mathcal{R}_i \mathcal{S}_i(2,2)\right|^2 + \left(1-M_{i+1}\right)^2 \left|1 - \mathcal{R}_i \mathcal{S}_i(2,1)\right|^2} \tag{6}$$

An equivalent expression can be derived when the downstream acoustic reflection coefficient $\mathcal{R}_{i+1}$ is known [5]. Without loss of generality, results will be solely presented in terms of the upstream acoustic reflection coefficient $\mathcal{R}_i$ in this work.

The acoustic response of a short circular hole sustaining a high Reynolds number, low Mach number bias flow is described here using two distinct models. The 2-step (2S) model, described in Sec. 3.1, corresponds to an isentropic area decrease followed by a non-isentropic area increase with large scale flow separation [5]. On the other hand, the quasi-steady Howe's (QSH) model, described in Sec. 3.2, corresponds to an hydrodynamically compact isentropic element where acoustic damping arises because of the coupling between unsteady vortical structures generated at the perforation rim and acoustic waves [6].

3.1 2-STEP (2S) MODEL

The 2-step (2S) model is a sequence of two more fundamental models. Viscous effects are assumed to be negligible across the cross section area contraction, between reference locations 1 and 2 in Fig. 1. As a consequence, the acoustic response of this subsystem is described through a transfer matrix $\mathcal{M}_{12}^{2S}$ corresponding to a low Mach isentropic area decrease [5]. On the other hand, large scale flow separation occurs at the sudden area expansion, between reference locations 2 and 3 in Fig. 1. Hence, this subsystem cannot be considered to be isentropic [2] and its acoustic response is described through a transfer matrix

Table 1. Expressions for the acoustic absorption coefficient Δ for various limiting cases.

Limiting case	2-step (2S) model	Quasi-steady Howe's (QSH) model
Anechoic boundary ($\mathcal{R}_1$=0)	$1-\frac{\left(1+4M_2\theta^{-1}\right)M_2^2\left(2-\theta^{-1}-\theta\right)^2+4}{\left(2-M_2\left(2-\theta^{-1}-\theta\right)\right)^2}$	$1-\frac{1+\left(1+4M_2\theta^{-1}\right)\left(M_2\theta\right)^2}{\left(1+M_2\theta\right)^2}$
Rigid boundary ($\mathcal{R}_1$=1)	0	0
Small hole ($\theta \gg 1$)	$1-\frac{\left\|2\mathcal{R}_1+M_2\left(2-\theta\right)\left(\mathcal{R}_1-1\right)\right\|^2+4}{\left\|2+M_2\left(2-\theta\right)\left(\mathcal{R}_1-1\right)\right\|^2+4\left\|\mathcal{R}_1\right\|^2}$	$1-\frac{\left\|\mathcal{R}_1\left(1-M_2\theta\right)+M_2\theta\right\|^2+1}{\left\|\mathcal{R}_1\right\|^2+\left\|1+M_2\theta\left(1-\mathcal{R}_1\right)\right\|^2}$
Large hole ($\theta \sim 1$)	$\frac{\left\|1-\mathcal{R}_1\right\|^2}{1+\left\|\mathcal{R}_1\right\|^2}M_2\left(\theta^{-1}+\theta-2\right)$	$\frac{\left\|1-\mathcal{R}_1\right\|^2}{1+\left\|\mathcal{R}_1\right\|^2}2M_2\theta$
No mean flow (M_2=0)	0	0

$\mathcal{M}_{23}^{2S}$ corresponding to a low Mach non-isentropic area increase with flow separation [5]. Both transfer matrices $\mathcal{M}_{12}^{2S}$ and $\mathcal{M}_{23}^{2S}$ depend on the Mach number inside the hole M_2 and the cross section area ratio θ only:

$$\mathcal{M}_{12}^{2S}=\begin{pmatrix}1 & M_2\left(\theta^{-1}-\theta\right)\\ 0 & \theta\end{pmatrix} \quad \left\| \quad \mathcal{M}_{23}^{2S}=\begin{pmatrix}1 & -2M_2\theta^{-1}\left(\theta^{-1}-1\right)\\ 0 & \theta^{-1}\end{pmatrix}\right. \tag{7}$$

The acoustic response of the system between reference locations 1 and 3 in Fig. 1 is then described through the transfer matrix $\mathcal{M}_{13}^{2S}=\mathcal{M}_{23}^{2S}\ \mathcal{M}_{12}^{2S}$. The acoustic response of short circular holes is represented using this approach in many low order network tools used for thermoacoustic stability prediction [2, 7]. The S-matrix $\mathcal{S}_{13}^{2S}$ describing the acoustic response of the whole system is then given by:

$$\mathcal{S}_{13}^{2S}=\frac{1}{2-M_2\left(2-\theta^{-1}-\theta\right)}\begin{pmatrix}2 & -M_2\left(2-\theta^{-1}-\theta\right)\\ -M_2\left(2-\theta^{-1}-\theta\right) & 2\end{pmatrix} \tag{8}$$

All terms of order M^2 and higher are neglected in Eq. (8). This expression is then inserted in Eq. (6), thus leading to:

$$\Delta^{2S}=1-\frac{\left(1+2M_2\theta^{-1}\right)\left|2\mathcal{R}_1+M_2\left(2-\theta^{-1}-\theta\right)\left(\mathcal{R}_1-1\right)\right|^2+4\left(1-2M_2\theta^{-1}\right)}{4\left(1+2M_2\theta^{-1}\right)\left|\mathcal{R}_1\right|^2+\left(1-2M_2\theta^{-1}\right)\left|2+M_2\left(2-\theta^{-1}-\theta\right)\left(\mathcal{R}_1-1\right)\right|^2} \tag{9}$$

Equation (9) is the expression of the acoustic absorption coefficient of a short circular hole sustaining a high Reynolds number, low Mach number bias flow according to the 2-step (2S) model for a given upstream acoustic boundary condition. Several limiting cases based on Eq. (9) and corresponding to upstream anechoic ($\mathcal{R}_1$=0) or rigid ($\mathcal{R}_1$=1) boundary conditions, small ($\theta \gg 1$) or large ($\theta \sim 1$) circular holes and the absence of a mean flow (M_2=0) are summarized in Table 1. The acoustic absorption coefficient Δ cancels out whenever M_2=0 or $\mathcal{R}_1$=1 for distinct reasons. For the first limiting case, there

is no source of acoustic damping because large scale flow separation does not occur in a quiescent fluid. On the other hand, when the upstream boundary reflection coefficient is equal to unity, the downstream boundary reflection coefficient is automatically equal to unity as well for the 2S model, this being due to the compactness assumption. As a consequence, all of the incoming acoustic energy is reflected at the system boundaries thus leading to the absence of acoustic damping.

3.2 QUASI-STEADY HOWE'S (QSH) MODEL

The quasi-steady Howe's (QSH) model is obtained from Howe's model, which quantifies the acoustic damping due to the conversion of acoustic energy into unsteady vortical energy across a short circular hole sustaining a high Reynolds number bias flow [6]. It is further assumed here that the incoming perturbations are hydrodynamically compact, e.g. that the Strouhal number $St \ll 1$. The expression for the transfer matrix representing the acoustic response of the system between reference locations 1 and 3 in Fig. 1 is simplified accordingly using a Puiseux series expansion for $St \to 0$. This simplified transfer matrix $\mathcal{M}_{13}^{QSH}$ and the associated S-matrix $\mathcal{S}_{13}^{QSH}$ are then given by:

$$\mathcal{M}_{13}^{QSH} = \begin{pmatrix} 1 & -2M_2\theta \\ 0 & 1 \end{pmatrix} \quad \Bigg\| \quad \mathcal{S}_{13}^{QSH} = \frac{1}{1+M_2\theta} \begin{pmatrix} 1 & M_2\theta \\ M_2\theta & 1 \end{pmatrix} \tag{10}$$

Once again, all terms of order M^2 and higher are neglected in Eq. (10). The expression for the S-matrix is then inserted in Eq. (6), thus leading to:

$$\Delta^{QSH} = 1 - \frac{\left(1+2M_2\theta^{-1}\right)\left|\mathcal{R}_1 + M_2\theta\left(1-\mathcal{R}_1\right)\right|^2 + \left(1-2M_2\theta^{-1}\right)}{\left(1+2M_2\theta^{-1}\right)\left|\mathcal{R}_1\right|^2 + \left(1-2M_2\theta^{-1}\right)\left|1+M_2\theta\left(1-\mathcal{R}_1\right)\right|^2} \tag{11}$$

Equation (11) is the expression of the acoustic absorption coefficient of a short circular hole sustaining a high Reynolds number, low Mach number bias flow according to the quasi-steady Howe's (QSH) model for a given upstream acoustic boundary condition. The same limiting cases as for the 2S model are derived based on Eq. (11) and summarized in Table 1. For the same reason as before, the acoustic absorption coefficient according to the QSH model cancels out when the upstream boundary reflection coefficient is equal to unity. Furthermore, the acoustic damping mechanism considered in the QSH model vanishes in the absence of a mean flow, thus leading to a zero acoustic absorption coefficient in that case.

4 RESULTS

The predictions for the acoustic absorption coefficient Δ of a short circular hole sustaining a high Reynolds number, low Mach number bias flow according to the 2S and QSH models are now discussed. Results for upstream anechoic boundary conditions $\mathcal{R}_1 = 0$ are represented as functions of the Mach number M_2 for various cross section area ratios θ in Fig. 2-(Left) and vice versa in Fig. 2-(Right). The solid and dotted lines represent the predictions according to the 2S and QSH models respectively.

For all θ and M_2 investigated, the predicted acoustic absorption coefficients lie between 0, corresponding to an unaffected acoustic energy balance, and 0.5, corresponding to a 50% reduction of the acoustic energy across the system. For limited cross section area ratios, corresponding to $\theta = 2$ and $\theta = 10$ in Fig. 2-(Left), Δ is larger for the QSH model compared to the 2S model for all Mach numbers M_2 investigated. Likewise, for limited Mach numbers, corresponding to $M_2 = 0.01$ in Fig. 2-(Right), Δ is larger for the QSH model compared to the 2S model for all cross section area ratios θ investigated. At larger Mach numbers M_2 (respectively cross section area ratios θ), there is a critical value of θ (respectively M_2) where the predictions according to the 2S model surpass those of the QSH model.

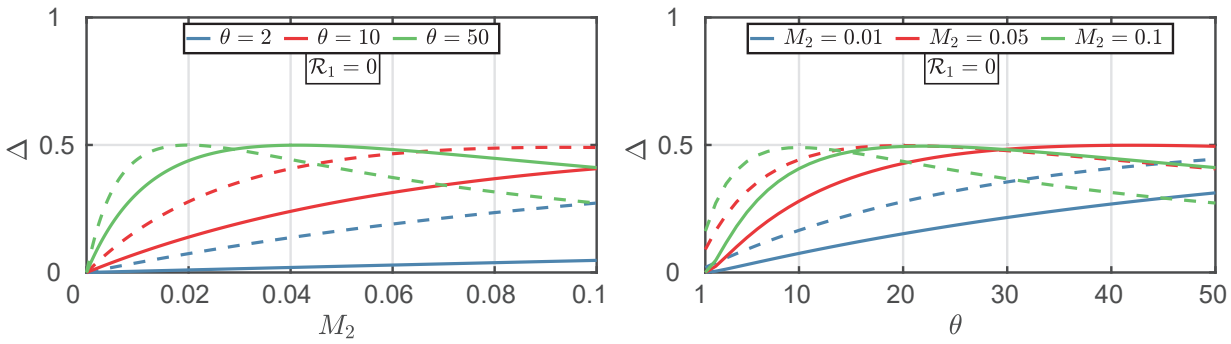

Figure 2. Acoustic absorption coefficient of a short circular hole sustaining a high Reynolds number, low Mach number bias flow for upstream anechoic boundary conditions as a function of M_2 for various θ (Left) and vice versa (Right). (Solid line): 2S model. (Dotted line): QSH model.

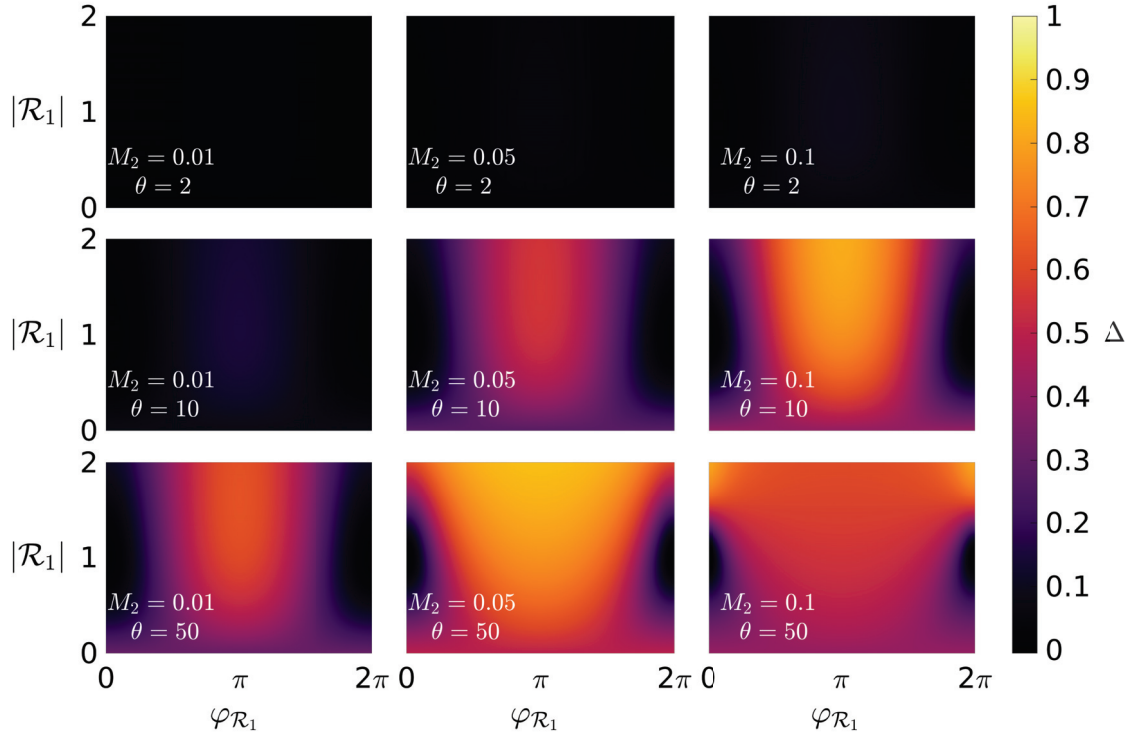

Figure 3. Acoustic absorption coefficient of a short circular hole sustaining a high Reynolds number, low Mach number bias flow according to the 2S model as a function of the phase (x-axis) and modulus (y-axis) of the upstream acoustic reflection coefficient $\mathcal{R}_1$. (Left) $M_1 = 0.01$ - (Center) $M_1 = 0.05$ - (Right) $M_1 = 0.1$. (Top) $\theta = 2$ - (Middle) $\theta = 10$ - (Bottom) $\theta = 50$.

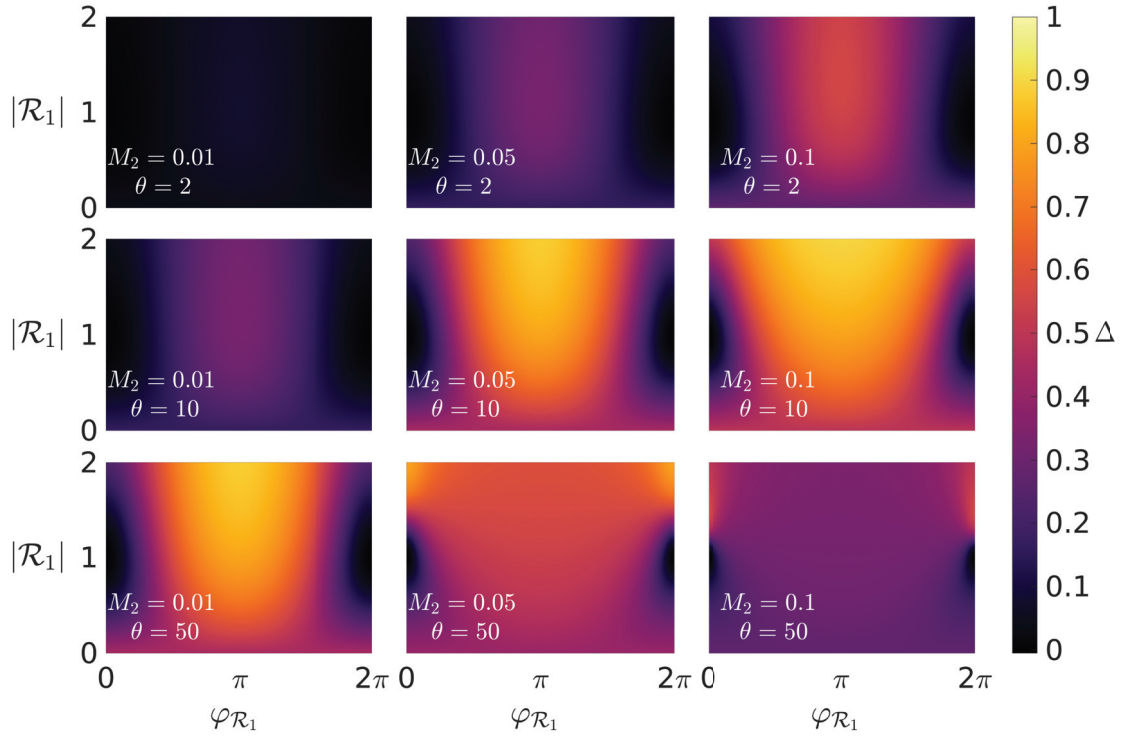

Figure 4. Acoustic absorption coefficient of a short circular hole sustaining a high Reynolds number, low Mach number bias flow according to the QSH model as a function of the phase (x-axis) and modulus (y-axis) of the upstream acoustic reflection coefficient $\mathcal{R}_1$. (Left) $M_1 = 0.01$ - (Center) $M_1 = 0.05$ - (Right) $M_1 = 0.1$. (Top) $\theta = 2$ - (Middle) $\theta = 10$ - (Bottom) $\theta = 50$.

The impact of the upstream acoustic reflection coefficient $\mathcal{R}_1$ on the acoustic absorption coefficient Δ is now investigated for the 2S model, as shown in Fig. 3, and for the QSH model, as shown in Fig. 4. For both models, three different Mach numbers M_2 and cross section area ratios θ are considered.

The evolution of the acoustic absorption coefficient as a function of the modulus and phase of the upstream acoustic reflection coefficient for given values of M_2 and θ are quite similar for the 2S and QSH models. For limited values of M_2 and θ, corresponding to Fig. 3-(Top Left) and Fig. 4-(Top Left), the acoustic absorption coefficient is close to zero whatever the acoustic reflection coefficient $\mathcal{R}_1$. For sizeable values of M_2 and θ, the acoustic absorption coefficient highly depends on both the modulus and phase of $\mathcal{R}_1$. The largest variations for the acoustic absorption coefficient according to the QSH model are observed for $M_2 = 0.1$ and $\theta = 10$ in Fig. 4-(Middle Right), where the minimum and maximum values of the acoustic absorption coefficient are respectively $\Delta^{QSH} \sim 0$ and $\Delta^{QSH} = 0.8988$. On the other hand, the largest variations for the acoustic absorption coefficient according to the 2S model are observed for $M_2 = 0.05$ and $\theta = 50$ in Fig. 3-(Bottom Center) with corresponding minimum and maximum values given by $\Delta^{2S} \sim 0$ and $\Delta^{2S} = 0.8581$ respectively. For both models, most of the acoustic energy entering the system is damped across the short circular hole for certain specific parameters. On the other hand, the acoustic energy balance is barely affected for other sets of parameters.

5 CONCLUSIONS

Analytical expressions for the acoustic absorption coefficient of a short circular hole sustaining a high Reynolds number, low Mach number bias flow were derived for two distinct models. In the first model, called the 2-step (2S) model, the acoustic response of the hole was represented using an isentropic area decrease followed by a non-isentropic area increase with large scale flow separation. In the second model, called the quasi-steady Howe's (QSH) model, the acoustic damping generated across the hole was described using Howe's model in the limit of small Strouhal numbers, corresponding to hydrodynamically compact perturbations. For both models, it was shown that the acoustic absorption coefficient was a function of the cross section area ratio θ, Mach number inside the hole M_2 and modulus and phase of the upstream acoustic reflection coefficient $\mathcal{R}_1$. Simplified expressions for the acoustic absorption coefficient were derived for both models for upstream anechoic boundary conditions $\mathcal{R}_1 = 0$ and for small ($\theta \gg 1$) and large ($\theta \sim 1$) holes. It was finally shown that the acoustic absorption coefficient was equal to zero for an upstream rigid boundary condition ($\mathcal{R}_1 = 1$) or in the absence of a mean flow ($M_2 = 0$) for both the 2S and QSH models.

The predictions of the acoustic absorption coefficient according to the 2S and QSH models were subsequently investigated. It was demonstrated that the impact of the upstream acoustic reflection coefficient $\mathcal{R}_1$ was limited for small values of the cross section area ratio θ and Mach number M_2. On the other hand, as M_2 or θ became sizable, the predicted acoustic absorption coefficient became highly dependent on the upstream acoustic reflection coefficient $\mathcal{R}_1$ for both models. For such conditions, the acoustic energy balance was shown to be unaffected for certain values of $\mathcal{R}_1$ while most of the acoustic energy was found to be damped across the system for other values of $\mathcal{R}_1$.

REFERENCES

[1] A. P. Dowling and A. S. Morgans. Feedback control of combustion oscillations. *Annu. Rev. Fluid Mech.*, 37(1):151–182, 2005.

[2] A. P. Dowling and S. R. Stow. Acoustic analysis of gas turbine combustors. *J. Propul. Power*, 19(5):751–764, 2003.

[3] R. Gaudron. *Acoustic response of premixed flames submitted to harmonic sound waves*. PhD thesis, Université Paris-Saclay, 2018.

[4] R. Gaudron, M. Gatti, C. Mirat, and T. Schuller. Impact of the acoustic forcing level on the transfer matrix of a turbulent swirling combustor with and without flame. *Flow Turbul. Combust.*, 2019.

[5] R. Gaudron and A. S. Morgans. Acoustic absorption in a subsonic mean flow at a sudden cross section area change. In *Proceedings of ICSV 26 – International Congress on Sound and Vibration*, pages 1–8, 2019.

[6] M. S. Howe. On the theory of unsteady high Reynolds number flow through a circular aperture. *Proc. R. Soc. Lond. A*, 366:205–223, 1979.

[7] J. Li, D. Yang, C. Luzzato, and A. Morgans. OSCILOS Report. Technical report, 2017.

[8] B. Massey. *Mechanics of Fluids*. Taylor & Francis, London, 2006.

[9] C. L. Morfey. Acoustic energy in non-uniform flows. *J. Sound Vib.*, 14(2):159–170, 1971.

[10] C. L. Morfey. Sound transmission and generation in ducts with flow. *J. Sound Vib.*, 14(1):37–55, 1971.

[11] M. L. Munjal. *Acoustics of ducts and mufflers*. John Wiley and Sons, Inc., New York, 1987.

[12] D. Potente. General design principles for an automotive muffler. In *Proceedings of Acoustics, 9-11 November 2005, Busselton, Western Australia*, 2005.

[13] S. F. Rehman and J. D. Eldredge. Numerical investigation of a bias-flow perforated liner for damping of thermoacoutic instabilities. In *Proceedings of GT2007, GT2007-27319*, 2007.

[14] G. A. Richards, D. L. Straub, and E. H. Robey. Passive Control of Combustion Dynamics in Stationary Gas Turbines. *J. Prop. Power*, 19(5):795–810, 2003.

[15] D. Yang and A. S. Morgans. The acoustics of short circular holes opening to confined and unconfined spaces. *J. Sound Vib.*, 393:41–61, 2017.